

Theory of magnetic structure in layered iridates: spin-orbit band or Mott insulators

Jean-Michel Carter¹ and Hae-Young Kee^{1,2,*}

¹*Department of Physics, University of Toronto, Toronto, Ontario M5S 1A7 Canada*

²*Canadian Institute for Advanced Research, Toronto, Ontario Canada*

In iridates, owing to strong spin-orbit coupling, the effective total angular momentum $j = 1/2$ band is well separated from the rest of the bands. In particular Sr_2IrO_4 (Sr-214) and $\text{Sr}_3\text{Ir}_2\text{O}_7$ (Sr-327) are magnetic insulators formed in $j = 1/2$ bands leading to an interesting proposal named spin-orbit Mott insulators. However, given that there is an even number of Ir atoms per unit cell due to a staggered rotation of octahedra and even number of layers, the non-interacting system could be a spin-orbit band insulator, questioning the Mott character in these materials. To answer the question on the nature of the insulating phases, and different states in various layered structures, we study a Hubbard model with a tight-binding spectrum designed for each Sr-214, Sr-327 and SrIrO_3 (Sr-113). A canted antiferromagnet (AF) is found in Sr-214 which is deep in the insulating phase close to strong coupling limit, while a collinear AF with c-axis moments is realized in Sr-327 near the spin-orbit band insulator. In contrast, Sr-113 is semimetallic. The origin of such a dissimilarity is explained, and implications of our results in relation to possible high temperature superconductors in doped iridates are further discussed.

PACS numbers: 71.30.+h, 71.70.Ej, 75.30.Kz

Introduction - Spin-orbit coupling (SOC) has often been either ignored or treated perturbatively in correlated electronic systems such as 3d- and 4d-orbital materials. However, with heavier atom systems, it becomes an important ingredient in determining the ground state of these materials and leads to novel phases such as topological insulators and spin liquids. In particular, when the SOC strength is comparable to the electronic interactions, understanding their interplay becomes challenging. Ir-oxides (iridates) with 5d-orbitals offer such a playground to investigate their combined effects.

It has been suggested that the effect of Hubbard interaction in iridates is amplified due to strong SOC via the narrowing of bandwidth, leading to an insulating state in some layered perovskite[1–26] and pyrochlore[27, 28] iridates. This state, called a spin-orbit Mott insulator, was first reported in single layered perovskite Sr_2IrO_4 (Sr-214).[6, 7, 9] An anisotropic Heisenberg spin model was derived at large U limit[8], and it was further proposed that anisotropic terms can be gauged away leading to an isotropic Heisenberg model of $j = 1/2$, reminiscent of the spin-1/2 undoped high temperature cuprates. Using this simple mapping, the idea of d-wave high temperature superconductivity in doped iridates was proposed.[14]

In this paper, we first question if the iridates are indeed Mott insulators and further investigate whether the mapping to the isotropic Heisenberg model for $j = 1/2$ is proper. To address these questions, we study a Hubbard model taking into account a tight binding Hamiltonian for the full unit cell. One important fact to notice is that in Sr-214 and Sr-327, there is an even number of Ir atoms due to the staggered IrO_6 octahedra rotation and four layers per unit cell. Thus according to the band theory, the non-interacting system could be a spin-orbit band insulator.

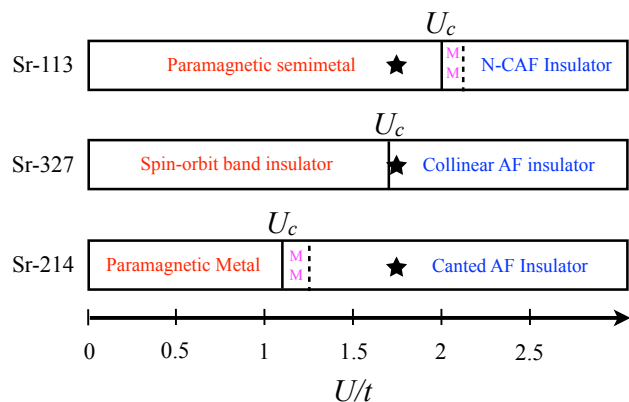


FIG. 1. [Color online] Phase diagram for the magnetic phases of the single layer, bilayer and 3D systems with the accompanying metal-insulator transition. The critical value of U of the magnetic transition for each system is $U_c/t = 1.07$, 1.72 and 1.98 respectively. For the Sr-214 and Sr-113 system, since the underlying band structure is metallic, the transition turns the metal into a magnetic metal (MM) before it develops a gap as the ordering increases. The ordered phases in the Sr-113 system is a non-coplanar canted AF (N-CAF), where the ferromagnetic moment points along the crystal c-axis. In a scenario where the Hubbard interaction is $1.73t \sim 0.5\text{eV}$ (setting $t \sim 300\text{meV}$), the stars represents where each system should be on the phase diagram.

We found that Sr-327 is indeed a band insulator at small U , which becomes a magnetic insulator as U increases. In contrast, Sr-214 is a metal at small U , which then turns into a magnetic metal and a magnetic insulator subsequently, while Sr-113 remains semimetal even at relatively large U as shown in Fig. 1.

A collinear AF with moments oriented along the crystal c-axis is found in Sr-327, while a coplanar canted AF is realized in Sr-214 as shown in Fig. 2. While the mag-

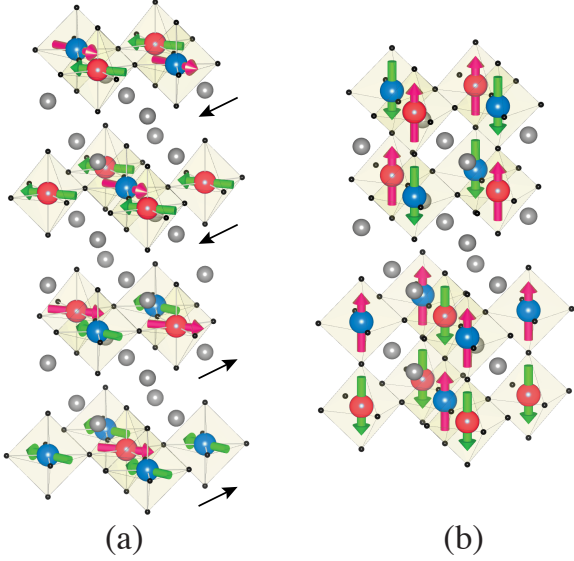


FIG. 2. [color online] Theoretical results of magnetic ordering in Sr-214 (a) and Sr-327 (b) in the insulating phase. Each layer has two different atoms because of the staggered rotation of the octahedra which we label blue and red. (a) The coplanar canted AF state is shown with the spin configuration displayed for each layers. The black arrow represents the direction of the ferromagnetic moment within the plane, showing the up-up-down-down structure. (b) The favored collinear AF state with moments pointing along the c-axis is shown where the second set of bilayer have its spins flipped from the first set.

netic ordering is certainly an effect of the interaction, it is not sufficient to conclude that iridates are Mott insulators in the strong U limit, where the charge gap due to electronic interaction should remain finite even when the magnetic order disappears. Can we distinguish weak U vs. strong U by studying their magnetic ordering patterns, which then act as a guide to understanding Mott insulators? We begin this study with a tight binding model.

Tight-binding model - A consistent description of the Ruddlesden-Popper series of strontium iridates can be achieved using a tight-binding model with on-site Hubbard interaction. Nearest in-plane and intra-bilayer hoppings (represented by t_p (t'_p) and t_z (t'_z) between same (different) j_z state, respectively), next-nearest (t_n), next-next-nearest (t_{nn}) neighbor hoppings, and nearest-inter-(bi)layer hoppings ($t_i, t_{id}, t_{iz}, t_{iy}$ and t_{ix}) in the $j = 1/2$ basis are included. Since both the Sr-214 and Sr-327 structures have four distinct layers per unit cell, and each layer has two different Ir atoms due to a staggered IrO_6 rotation, it is convenient to introduce the following spinor basis: $\psi_k^\alpha = (c_{k\uparrow}^{\alpha B}, c_{k\downarrow}^{\alpha B}, c_{k\uparrow}^{\alpha R}, c_{k\downarrow}^{\alpha R})$, where $\alpha = 1, \dots, 4$ is the layer index, B(R) is the sublattice label representing alternating IrO_6 rotation, and arrows denote $j_z = \pm 1/2$.

Since we only consider hoppings between neighboring

layers, the Hamiltonian can be written in general as $H = \sum_k \psi_k^{\alpha\dagger} H_k^{\alpha\beta} \psi_k^\beta + U \sum_i c_{i\uparrow}^\dagger c_{i\downarrow}^\dagger c_{i\downarrow} c_{i\uparrow}$, where

$$H_k^{\alpha\beta} = \begin{pmatrix} A_k & B_k & 0 & e^{ik_z c} C_k^\dagger \\ B_k^\dagger & A_k & C_k & 0 \\ 0 & C_k^\dagger & A_k & B_k \\ e^{-ik_z c} C_k & 0 & B_k^\dagger & A_k \end{pmatrix}, \quad (1)$$

and U is the on-site Hubbard interaction in j -basis. Note that in addition to bandwidth effects, the Hubbard interaction U is renormalized by a factor of $1/3$ from \tilde{U} of the orbital basis, due to basis change from the orbital basis to the j basis (i.e., $U = \tilde{U}/3$). Here, A_k , B_k , and C_k are 4×4 matrices with A_k containing intra-layer hoppings only, B_k contains hoppings between layers 1 and 2 (3 and 4) and C_k contains hoppings between layers 2 and 3 (4 and 1 where c is a c -axis lattice constant). Since A_k is within a given layer, it is the same for both the single-layer and bilayer systems.

The main difference between the single-layer and the bilayer system is the coupling between layers 1 and 2 (and 3 and 4), B_k . In the single-layered version, this coupling is weak and each atom is coupled with 4 atoms of the next layer (because of the c -axis stacking) whereas it is strong in the bilayer Sr-327. Note that R (B) is sitting on top of B (R), which differs from Sr-214. This is responsible for the different magnetic ordering patterns for these two layered iridates, which we will discuss further below.

For both the single layer and the bilayer system, the coupling between layers 2 and 3 (and 4 and 1) are nearly identical due to the similarities between the inter-layer structures with layer 3 being displaced from layer 2 by half a planar lattice vector (110 or $1\bar{1}0$). We therefore allow the C_k matrices for both system to be identical. In Sr-214, the small difference between B_k and C_k is due to the difference in displacement between neighboring layers. Between layers 1 and 2, the displacement is half the lattice vector (110) whereas it is half the lattice vector ($1\bar{1}0$) between layers 2 and 3. All the forms of A_k , B_k and C_k which include the dispersions and hopping parameters derived using Slater-Koster theory are given in the supplementary materials.

Mean-Field Theory - Given the tight binding Hamiltonian, we then treat the Hubbard interaction at the mean-field (MF) level to find possible magnetic orderings. Performing a MF decoupling in the magnetic channel, the interaction is written as,

$$H_{int} = -\frac{2U}{3} (S_{ix}^2 + S_{iy}^2 + S_{iz}^2) + \frac{U}{2} \sum_i (n_{i\uparrow} + n_{i\downarrow}) \quad (2)$$

where we take $S_{i\alpha}^2 = 2m_{i\alpha}S_{i\alpha} - m_{i\alpha}^2$ and compute $m_{i\alpha}$ self-consistently. There are 24 order parameters from 4 layers, 2 sublattices, and 3 directions of \mathbf{m} for Sr-214 and Sr-327. In SrIrO_3 (Sr-113), there are 12 order parameters for 4 sublattices and 3 directions of \mathbf{m} . As U

increases, there is a second order phase transition from metal/semimetal/band insulator into a magnetically ordered phase as shown in Fig. 1. Below we discuss some details of phase diagram for each system.

For Sr-214, the magnetic ordering occurs at $U_c = 1.07t$, where t is the magnitude of the Slater-Koster hopping $t_{dd\pi}$ and used as the energy scale throughout the remainder of the paper. The canted AF is the ground state. In addition, the direction of the net ferromagnetic component is also determined to be either in the (110) direction or the (1 $\bar{1}$ 0) direction in an up-up-down-down (110) or up-down-down-up (1 $\bar{1}$ 0) pattern along the c-axis as shown in Fig. 2. This magnetic ordering pattern remains unchanged in the large U -limit, and is consistent with the experimental results obtained by resonant x-ray scattering techniques.[1, 3, 6, 9]

For Sr-327, when $U < U_c = 1.72t$, one has a spin-orbit band insulator. It then becomes a magnetic insulator, where the charge gap increases gradually across the second order transition. Note that there are five B Ir-atoms surrounding R Ir-atom in Sr-327. The competition between canted AF and collinear AF strongly depends on the in-plane and z-axis bilayer hoppings. We found that only when the ratio of t'_z/t_z is close to the ratio of t'_p/t_p , the degeneracy of canted AF and collinear AF persists. We estimate $t'_z/t_z \approx 3 t'_p/t_p$ for Sr-327 based on Slater-Koster theory, leading to a collinear AF state along the c-axis favored by the bilayer coupling. Such a state has been recently confirmed in experiments[20, 21, 23, 26]. The canted AF state can become a lower energy state when the inter-layer couplings (C_k) are enhanced, but only in an unrealistic limit, or when the ratio between t'_z/t_z and t'_p/t_p is very close to 1. Due to the two sets of bilayers per unit cell, 2 different configurations with almost degenerate energies are possible in the collinear AF ground state. One (with a slightly lower energy) is shown in Fig. 2 (b), and another spin configuration is equivalent to having the opposite spins on the 2nd bilayer set. These two configurations were experimentally observed in ref. [23].

The difference in energy between the collinear AF state and the coplanar canted AF state can be used here to estimate the spin gap reported by resonant inelastic x-ray scattering (RIXS) techniques. For the set of parameters given in the supplementary material, the difference in energy between the 2 states per Ir atom for $U/t = 2$ is of the order of $3 \times 10^{-4}t$. Approximating the Slater-Koster hopping $|t_{dd\pi}| = 300\text{meV}$, we get a spin gap which is approximately 0.1 meV, two orders of magnitude smaller than the 90meV gap[21]. This result seems to indicate a small spin gap, which may be hidden within the resolution of the RIXS data.

The same mean-field approach can be used on the orthorhombic perovskite Sr-113 model described in [18]. In this case, because of the tilting of the octahedra (in addition to the rotation), a non-coplanar canted AF magnetic

ordering occurs, but with the canted moment pointing along the z-direction instead of in the plane. The mean-field transition occurs at $U_c = 1.98t$ in this case, and the Hubbard repulsion in iridates should be $\sim 1.73t$ corresponding to $\sim 0.5\text{eV}$.

Large- U limit spin model - We found that the magnetic structures do not change with a large U in our MF study. To understand how the above weak coupling results are related to the strong coupling approach, we derive a spin model in the large U limit. Within a second order perturbation theory, the Heisenberg, Dzyaloshinskii-Moriya (DM) and anisotropic exchange terms are obtained as follows. For a general time reversal symmetric hopping between two sites given by $(t_{\alpha\beta} + i\vec{\sigma} \cdot \vec{v}_{\alpha\beta})c_{i,\alpha\sigma}^\dagger c_{j,\beta\sigma'}$, the spin-model is

$$H = \sum_{\langle ij \rangle > \alpha\beta} \left(J_{ij}^{\alpha\beta} \vec{S}_i^\alpha \cdot \vec{S}_j^\beta + \vec{D}_{ij}^{\alpha\beta} \cdot \vec{S}_i^\alpha \times \vec{S}_j^\beta + \vec{S}_i^\alpha \cdot \Gamma_{ij}^{\alpha\beta} \cdot \vec{S}_j^\beta \right). \quad (3)$$

Here $J_{ij}^{\alpha\beta} = \frac{4}{U}(t_{\alpha\beta}^2 - v_{\alpha\beta}^2)$, $\vec{D}_{ij}^{\alpha\beta} = \frac{4}{U}(2t_{\alpha\beta}\vec{v}_{\alpha\beta})$, and the anisotropic exchange $\Gamma_{ij,ab}^{\alpha\beta} = \frac{4}{U}(2v_{\alpha\beta}^a v_{\alpha\beta}^b)$ where a, b are spin components and $\alpha\beta$ are layer indices. Note that these exchange terms depend not only on site i, j but also on layer index and spin component. The in-plane nearest-neighbor exchange can be written as $J_{BR}^{\alpha\alpha} = \frac{4(t_p^2 - t_z^2)}{U}$, $\vec{D}_{BR}^{\alpha\alpha} = \frac{8\varepsilon_i t_p t'_p}{U} \hat{z}$ and $\Gamma_{BR,zz}^{\alpha\alpha} = \frac{8t_p'^2}{U}$ and are the same for Sr-214 and Sr-327, for $\alpha = 1, \dots, 4$ leading to a degeneracy between canted AF and collinear AF if the inter-layer terms are ignored.

For Sr-214, the exchange terms between layers 1 and 2 is found to be $J_{BB}^{12} = \frac{4t_i^2}{U}$, $J_{BR}^{12} = \frac{4}{U}(t_{id}^2 - t_{iz}^2 - t_{iy}^2 - t_{ix}^2)$, $D_{BR}^{12} = \frac{8}{U}(\pm t_{id}t_{ix}, \pm t_{id}t_{iy}, t_{id}t_{iz})$ with

$$\Gamma_{BR}^{12} = \frac{8}{U} \begin{pmatrix} t_{ix}^2 & t_{ix}t_{iy} & \pm t_{ix}t_{iz} \\ t_{ix}t_{iy} & t_{iy}^2 & \pm t_{iy}t_{iz} \\ \pm t_{ix}t_{iz} & \pm t_{iy}t_{iz} & t_{iz}^2 \end{pmatrix},$$

where t_i represents inter-layer hopping integral between B and B (or R and R), while t_{id} between B and R. The spin σ_a -dependent hopping term between B and R are denoted by t_{ia} where $a = x, y, z$. The \pm denotes the sign change in the two σ_x - and σ_y -dependent hoppings between B(R) in layer 1 and the two R(B) in layer 2 it connects to. Because of the sign changes, these terms have effectively no effect if the magnetic unit cell is the same as the lattice unit cell. The exchange terms between layers 2 and 3 are identical except for the y -component of the DM-term where $D_{BR}^{23,y} = -D_{BR}^{12,y}$ and the xy - and yz -components of the anisotropic exchange where $\Gamma_{BR}^{23,xy} = -\Gamma_{BR}^{12,xy}$ and $\Gamma_{BR}^{23,yz} = -\Gamma_{BR}^{12,yz}$.

The isotropic term by itself would favor a collinear AF state, but it is largely frustrated due to the fact that each atom is coupled with 4 atoms of each neighboring layers. The same applies to the DM-vectors but the anisotropic exchange term Γ_{xy} on the other hand favors the canted

AF state in an up-up-down-down configuration. Due to the reduced effect of the other terms because of the lattice structure, the anisotropic exchange is large enough to have the canted AF be the ground state. It has been shown [8] that the Hund's coupling and tetragonal distortion also favor the canted AF state, further stabilizing this state.

For Sr-327, the in-plane spin exchange are identical to those for the single layer. In addition, the bilayer exchange are given by $J_{BR}^{12} = \frac{4}{U}(t_z^2 - t_z'^2)$, $\bar{D}_{BR}^{12} = \epsilon_i \frac{8}{U} t_z t_z' \hat{z}$ and $\Gamma_{BR,zz}^{12} = \frac{8}{U} t_z'^2$. Note that unless $t_z'/t_z = t_p'/t_p$, the DM interaction in-plane and out-of-plane are frustrated, i.e. it is impossible to configure the spins such that the optimal canting is achieved both in-plane and within the two layers. Thus, the collinear AF state is the ground state, due to the opposite rotation of the octahedra between adjacent layers, consistent with the bilayer spin model results discussed in Ref. [20].

Adding the inter-layer hoppings, the c-axis stacking favors an AF pattern between the same atom of layers 2 and 3 as seen in Fig. 2, but the ferromagnetic pattern is very close in energy, leading to the two possible arrangements discussed previously.

Discussion and summary - We offer a systematic study for different layered iridates using a Hubbard model that captures a rich phase diagram; metal to magnetic metal to magnetic insulator for Sr-214, band insulator to magnetic insulator for Sr-327, and semimetal to magnetic semimetal to magnetic insulator for Sr-113, as U increases. The ground state magnetic ordering patterns are sensitive to the lattice structure. In Sr-214, the inter-layer isotropic Heisenberg and DM interactions are frustrated, because Ir atom in adjacent layers have zero effective field due to their position. This effect, combined with the anisotropic exchange term, selects the “up-up-down-down” pattern for the net ferromagnetic moment pointing in (110)- or (1 $\bar{1}$ 0)-direction. On the other hand, the bilayer lattice structure frustrates the DM interaction of the 5 neighbors of each Ir atom making the collinear AF state along the c-axis the preferred configuration in Sr-327, in contrast with Sr-214. However, the canted AF is close in energy, making the spin dynamics, temperature and magnetic field dependence interesting subjects for future study.

For all the iridates studied here, magnetic ordering structures are identical to those for large U limit obtained by the spin model, implying that their Mott character cannot be corroborated by the magnetic ordering. However, Sr-214 is far from its metal-insulator transition, deep in the insulating phase, while Sr-327 is nearby a small gap band insulator at $U \sim 0.5\text{eV}$ suggesting that the magnetic ordering does not support a Mott insulator. We suggest that ARPES study below and above the transition temperature to test our proposal.

A comparison to cuprates deserves some discussion. Given that $j = 1/2$ spin model resembles the high tem-

perature cuprates of spin $1/2$, a possibility of achieving d-wave high temperature superconductivity in doped iridates became appealing. However, the essential difference is that the $j = 1/2$ wavefunction is made of equal mixture of the t_{2g} orbitals, leading to an isotropic s-wave-like wavefunction while the two dimensional $d_{x^2-y^2}$ orbital is a basic ingredient of the cuprates. This results in a strong bilayer coupling in Sr-327 at the origin of the spin-orbit band insulator at small U regime, making this system distinct from bilayer cuprates where the bilayer coupling can be treated perturbatively. Along similar lines, the anisotropic exchange terms are not negligible and the proposed d-wave pairing in doped iridates will be unlikely achieved, even though superconductivity is still an open possibility.

Acknowledgement - This work was supported by NSERC of Canada. HYK acknowledges the Aspen Center for Physics where a part of the work was carried out.

* hykee@physics.utoronto.ca

- [1] M. K. Crawford, M. A. Subramanian, R. L. Harlow, J. A. Fernandez-Baca, Z. R. Wang, and D. C. Johnston, Phys. Rev. B **49**, 9198 (1994).
- [2] Q. Huang, J. Soubeyroux, O. Chmaissem, I. Sora, A. Santoro, R. Cava, J. Krajewski, and W. P. Jr., Journal of Solid State Chemistry **112**, 355 (1994).
- [3] G. Cao, J. Bolivar, S. McCall, J. E. Crow, and R. P. Guertin, Phys. Rev. B **57**, R11039 (1998).
- [4] G. Cao, Y. Xin, C. S. Alexander, J. E. Crow, P. Schlottmann, M. K. Crawford, R. L. Harlow, and W. Marshall, Phys. Rev. B **66**, 214412 (2002).
- [5] I. Nagai, Y. Yoshida, S. I. Ikeda, H. Matsuhata, H. Kito, and M. Kosaka, Journal of Physics: Condensed Matter **19**, 136214 (2007).
- [6] B. J. Kim, H. Jin, S. J. Moon, J.-Y. Kim, B.-G. Park, C. S. Leem, J. Yu, T. W. Noh, C. Kim, S.-J. Oh, J.-H. Park, V. Durairaj, G. Cao, and E. Rotenberg, Phys. Rev. Lett. **101**, 076402 (2008).
- [7] S. J. Moon, H. Jin, K. W. Kim, W. S. Choi, Y. S. Lee, J. Yu, G. Cao, A. Sumi, H. Funakubo, C. Bernhard, and T. W. Noh, Phys. Rev. Lett. **101**, 226402 (2008).
- [8] G. Jackeli and G. Khaliullin, Phys. Rev. Lett. **102**, 017205 (2009).
- [9] B. J. Kim, H. Ohsumi, T. Komesu, S. Sakai, T. Morita, H. Takagi, and T. Arima, Science **323**, 1329 (2009).
- [10] S. Chikara, O. Korneta, W. P. Crummett, L. E. DeLong, P. Schlottmann, and G. Cao, Journal of Applied Physics **107**, 090000 (2010), arXiv:0908.0773 [cond-mat.str-el].
- [11] H. Jin, H. Jeong, T. Ozaki, and J. Yu, Phys. Rev. B **80**, 075112 (2009).
- [12] S. J. Moon, H. Jin, W. S. Choi, J. S. Lee, S. S. A. Seo, J. Yu, G. Cao, T. W. Noh, and Y. S. Lee, Phys. Rev. B **80**, 195110 (2009).
- [13] L. J. P. Ament, G. Khaliullin, and J. van den Brink, Phys. Rev. B **84**, 020403 (2011).
- [14] F. Wang and T. Senthil, Physical Review Letters **106**, 136402 (2011).
- [15] H. Watanabe, T. Shirakawa, and S. Yunoki, Phys. Rev.

- Lett. **105**, 216410 (2010).
- [16] M. Ge, T. F. Qi, O. B. Korneta, D. E. De Long, P. Schlottmann, W. P. Crummett, and G. Cao, Phys. Rev. B **84**, 100402 (2011).
 - [17] C. Martins, M. Aichhorn, L. Vaugier, and S. Biermann, Phys. Rev. Lett. **107**, 266404 (2011).
 - [18] J.-M. Carter, V. V. Shankar, M. A. Zeb, and H.-Y. Kee, Phys. Rev. B **85**, 115105 (2012).
 - [19] S. Boseggia, R. Springell, H. C. Walker, A. T. Boothroyd, D. Prabhakaran, D. Wermeille, L. Bouchenoire, S. P. Collins, and D. F. McMorrow, Phys. Rev. B **85**, 184432 (2012).
 - [20] J. W. Kim, Y. Choi, J. Kim, J. F. Mitchell, G. Jackeli, M. Daghofer, J. van den Brink, G. Khaliullin, and B. J. Kim, ArXiv e-prints (2012), arXiv:1205.4381 [cond-mat.str-el].
 - [21] J. Kim, A. H. Said, D. Casa, M. H. Upton, T. Gog, M. Daghofer, G. Jackeli, J. van den Brink, G. Khaliullin, and B. J. Kim, ArXiv e-prints (2012), arXiv:1205.5337 [cond-mat.str-el].
 - [22] J. P. Clancy, N. Chen, C. Y. Kim, W. F. Chen, K. W. Plumb, B. C. Jeon, T. W. Noh, and Y.-J. Kim, ArXiv e-prints (2012), arXiv:1205.6540 [cond-mat.str-el].
 - [23] S. Boseggia, R. Springell, H. Walker, A. Boothroyd, D. Prabhakaran, S. Collins, and D. McMorrow, ArXiv e-prints (2012), arXiv:1207.0173 [cond-mat.str-el].
 - [24] C. Dhital, S. Khadka, Z. Yamani, C. de la Cruz, T. C. Hogan, S. M. Disseler, M. Pokharel, K. C. Lukas, W. Tian, C. P. Opeil, Z. Wang, and S. D. Wilson, ArXiv e-prints (2012), arXiv:1206.1006 [cond-mat.str-el].
 - [25] M. Ahsan Zeb and H.-Y. Kee, ArXiv e-prints (2012), arXiv:1206.5836 [cond-mat.str-el].
 - [26] J. P. Clancy, K. W. Plumb, C. S. Nelson, Z. Islam, G. Cao, T. Qi, and Y.-J. Kim, ArXiv e-prints (2012), arXiv:1207.0960 [cond-mat.str-el].
 - [27] D. Pesin and L. Balents, Nat Phys **6**, 376 (2010).
 - [28] B.-J. Yang and Y. B. Kim, Phys. Rev. B **82**, 085111 (2010).
 - [29] B. M. Wojek, M. H. Berntsen, S. Boseggia, A. T. Boothroyd, D. Prabhakaran, D. F. McMorrow, H. M. Rønnow, J. Chang, and O. Tjernberg, ArXiv e-prints (2012), arXiv:1207.1556 [cond-mat.str-el].

SUPPLEMENTARY MATERIAL

Hopping parameters and dispersions

The intra-layer hopping matrix is given as

$$A_k = \epsilon_k^a + \epsilon_k^{ad} \tau_x + \epsilon_k'^{ad} \tau_y \sigma_z, \quad (4)$$

where τ represents the sublattice degree of freedom and σ represents the spin. The dispersions obtained using the symmetry of the hopping parameters are given as

$$\begin{aligned} \epsilon_k^a &= 4t_n \cos(k_x) \cos(k_y) + 2t_{nn}(\cos(2k_x) + \cos(2k_y)) \\ \epsilon_k^{ad} &= 2t_p(\cos(k_x) + \cos(k_y)) \\ \epsilon_k'^{ad} &= 2t'_p(\cos(k_x) + \cos(k_y)), \end{aligned}$$

with the hopping parameters listed in Table I.

The first inter-layer hopping matrix given by

$$\begin{aligned} B_{1k} &= \epsilon_k^b + \epsilon_k^{bd} \tau_x + \epsilon_k^{bz} \tau_y \sigma_z + \epsilon_k^{by} \tau_y \sigma_y + \epsilon_k^{bx} \tau_y \sigma_x, \\ B_{2k} &= t^z \tau_x + t'_z \tau_y \sigma_z \end{aligned} \quad (5)$$

where B_{1k} is for the Sr-214 system with weak inter-layer hoppings and B_{2k} is for the Sr-327 system with strong bilayer coupling. The dispersions for the inter-layer couplings in matrix B_{1k} are given by

$$\begin{aligned} \epsilon_k^b &= 2t_i \cos((k_x + k_y)/2) \\ \epsilon_k^{bd} &= 2t_{id} \cos((k_x - k_y)/2) \\ \epsilon_k^{bz} &= 2t_{iz} \cos((k_x - k_y)/2) \\ \epsilon_k^{by} &= i2t_{iy} \sin((k_x - k_y)/2) \\ \epsilon_k^{bx} &= i2t_{ix} \sin((k_x - k_y)/2), \end{aligned}$$

whereas B_{2k} doesn't have a dispersion since the B(R) atom from layer 2 sits on top of the R(B) atom of layer 1.

Finally, the second inter-(bi)layer hopping matrix is given by

$$C_k = \epsilon_k^c + \epsilon_k^{cd} \tau_x + \epsilon_k^{cz} \tau_y \sigma_z + \epsilon_k^{cy} \tau_y \sigma_y + \epsilon_k^{cx} \tau_y \sigma_x, \quad (6)$$

with the dispersions given by

$$\begin{aligned} \epsilon_k^c &= 2t_i \cos((k_x - k_y)/2) \\ \epsilon_k^{cd} &= 2t_{id} \cos((k_x + k_y)/2) \\ \epsilon_k^{cz} &= 2t_{iz} \cos((k_x + k_y)/2) \\ \epsilon_k^{cy} &= -i2t_{iy} \sin((k_x + k_y)/2) \\ \epsilon_k^{cx} &= i2t_{ix} \sin((k_x + k_y)/2). \end{aligned}$$

The hopping parameters for B_{1k} and C_k are listed in Table I.

All the hopping parameters were derived using Slater-Koster hoppings for d-electrons with $(t_{dd\pi}, t_{dd\sigma}, t_{dd\delta}) = (-1, 3/2, 1/4)$ for nearest neighbor hoppings, and setting

TABLE I. List of intra-layer hopping parameters and list of bilayer and inter-(bi)layer hopping parameters in unit of t

t_p			t'_p			t_n	t_{nn}
-0.57			-0.10			0.005	-0.01
t_z	t'_z	t_i	t_{id}	t_{iz}	t_{iy}	t_{ix}	
-0.46	-0.23	-0.029	-0.0275	-0.0135	-0.0095	0.0095	

the ratios between next-nearest-neighbor and nearest-neighbor hoppings to be $r = 0.2$ and between next-next-nearest neighbor and nearest-neighbor to be $r' = 0.02$. We also used the ratio between inter-(bi)layer hopping to nearest-neighbor hopping to be $r'' = 0.1$.

Note that bilayer hoppings t_z and t'_z are relatively similar to the in-plane hoppings of t_p and t'_p , respectively. As we discussed in the main text, this is inherited from the character of $j = 1/2$ wavefunction containing equal weights of d_{xz} , d_{yz} in addition to d_{xy} orbitals. This combination of $j = 1/2$ wavefunction also leads to an extremely small next nearest neighbor hopping t_n in the plane. There are three orbital hopping contributions along the diagonal directions between B to B (or R to R). One is from d_{xy} to d_{xy} orbitals whose hopping integral is positive, and it is σ -type. On the other hand, d_{xz} to d_{xz} and d_{yz} to d_{yz} orbital hopping integrals are π -type and comes negative. These two type hopping integrals nearly cancel each other, and leave only a small strength of t_n . The octahedra rotation makes the d_{xy} hopping even smaller, which decreases t_n further.

Charge gap and magnetic moment

Given the set of tight-binding parameters listed above, the Sr-327 system displays an underlying insulating band structure shown in Fig. 3 below. The direct gaps near X and M depend mainly on the in-plane and bilayer hoppings (t_p , t'_p , t_z and t'_z), and the overall dispersion also depends on the next-nearest in-plane neighbor hopping (t_n).

While bilayer hoppings are necessary to open a direct gap, a large value of t_n could push the bottom of the band near M further down, and push up the top of band near X further up in such a way that small electron and hole pockets at the X and M points could appear. These band touchings occurs when $t_n = 0.047$ assuming that the other parameters are fixed. For the reason discussed the above, t_n greater than 0.01 would be unrealistic and thus the insulating structure will be robust for the small U regime.

We also note that the magnetic moment of Sr-327 is about $0.03\mu_B$ [4], which is close to our order parameter at $U = 1.73t$ in Sr-327. This small order parameter should not affect the charge gap much, but the charge gap re-

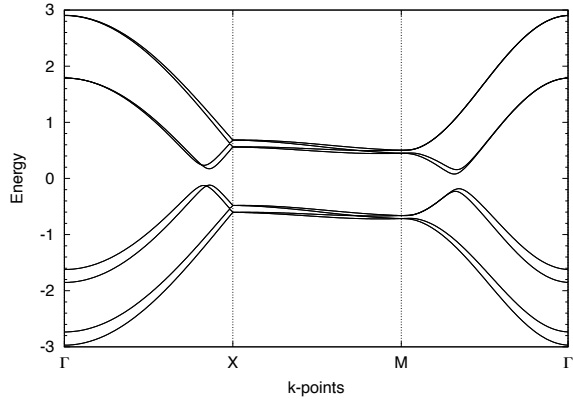


FIG. 3. Underlying band structure for the Sr-327 model. This system is a “spin-orbit band insulator” at small U and a magnetic transition occurs which opens the band gap further as U increases

ported by a recent ARPES is of the order of 100 meV[29]. Therefore, this sizeable charge gap must originate mainly from the underlying band gap, especially because the correlation is not strong in Sr-327 as we shown in the current study.